

# Diagnosing Heteroskedasticity and Resolving Multicollinearity Paradoxes in Physicochemical Property Prediction

Malikussaid

*School of Computing, Telkom University  
Bandung, Indonesia*

malikussaid@student.telkomuniversity.ac.id

Septian Caesar Floresko

*School of Computing, Telkom University  
Bandung, Indonesia*

Ade Romadhyony

*School of Computing, Telkom University  
Bandung, Indonesia*

aderomadhyony@telkomuniversity.ac.id

Isman Kurniawan

*School of Computing, Telkom University  
Bandung, Indonesia*

ismankrn@telkomuniversity.ac.id

Warih Maharani

*School of Computing, Telkom University  
Bandung, Indonesia*

wmahrani@telkomuniversity.ac.id

Hilal Hudan Nuha

*School of Computing, Telkom University  
Bandung, Indonesia*

hilalnuha@telkomuniversity.ac.id

**Abstract**—Lipophilicity (logP) prediction remains central to drug discovery, yet linear regression models for this task frequently violate statistical assumptions in ways that invalidate their reported performance metrics. We analyzed 426,850 bioactive molecules from a rigorously curated intersection of PubChem, ChEMBL, and eMolecules databases, revealing severe heteroskedasticity in linear models predicting computed logP values (XLOGP3): residual variance increases 4.2-fold in lipophilic regions (logP greater than 5) compared to balanced regions (logP 2 to 4). Classical remediation strategies—Weighted Least Squares and Box-Cox transformation—failed to resolve this violation (Breusch-Pagan p-value less than 0.0001 for all variants). Tree-based ensemble methods (Random Forest R-squared of 0.764, XGBoost R-squared of 0.765) proved inherently robust to heteroskedasticity while delivering superior predictive performance. SHAP analysis resolved a critical multicollinearity paradox: despite a weak bivariate correlation of 0.146, molecular weight emerged as the single most important predictor (mean absolute SHAP value of 0.573), with its effect suppressed in simple correlations by confounding with topological polar surface area (TPSA). These findings demonstrate that standard linear models face fundamental challenges for computed lipophilicity prediction and provide a principled framework for interpreting ensemble models in QSAR applications.

**Keywords**—heteroskedasticity, multicollinearity, SHAP, lipophilicity prediction, QSAR, ensemble methods

## I. INTRODUCTION

Lipophilicity, quantified as the logarithm of the octanol-water partition coefficient (logP), governs multiple absorption, distribution, metabolism, excretion, and toxicity (ADMET) parameters in drug discovery [1]. Its inclusion in Lipinski’s “Rule of Five” [2] established it as a fundamental filter for oral bioavailability, and contemporary AI-driven drug design continues to optimize this property actively [3]. Computational prediction of lipophilicity from molecular structure remains an active research area, with applications ranging from virtual screening to lead optimization, though challenges persist in achieving both accuracy and statistical interpretability.

The proliferation of large public chemical databases—PubChem [4], [5], [6], ChEMBL [7], [8], [9], [10], and commercial repositories like eMolecules [11]—has enabled the construction of massive training datasets. Yet scale alone does not guarantee model validity. Recent perspectives from domain experts emphasize that “poor data quality is a major concern with the rise of machine learning” methods, as

aggregation can propagate errors into computational models [12]. Furthermore, while modern machine learning achieves impressive predictive performance, statistical assumptions underpinning model interpretation are frequently overlooked.

This study addresses three critical gaps in current QSAR methodology for lipophilicity prediction using computed logP values. First, we demonstrate that linear regression models—despite numerically acceptable  $R^2$  values—violate the homoskedasticity assumption in a systematic, chemically meaningful pattern that invalidates their statistical inferences. Second, we document the failure of representative classical remediation strategies (Weighted Least Squares, target transformation) to resolve this violation. Third, we employ SHAP (SHapley Additive exPlanations) [13] to resolve an apparent multicollinearity paradox where molecular weight (MolWt) shows negligible bivariate correlation with computed logP ( $r = 0.146$ ) yet emerges as the single most important predictor in multivariate models.

Our analysis utilized a rigorously curated dataset of 426,850 bioactive molecules obtained from the intersection of three authoritative databases, with computed lipophilicity values from PubChem’s XLOGP3 algorithm serving as the prediction target. We demonstrate that tree-based ensemble methods (Random Forest [14], XGBoost [15]) are inherently robust to heteroskedasticity and achieve superior performance ( $R^2 = 0.765$ , RMSE = 0.731 logP units) compared to regularized linear models ( $R^2 = 0.608$ , but statistically unreliable). The SHAP analysis reveals that the weak MolWt correlation is a suppression artifact caused by MolWt’s confounding with topological polar surface area (TPSA), and that controlling for this confound unmasks MolWt as the dominant predictor. These findings provide actionable guidance for both model selection and feature interpretation in computational physicochemical property prediction.

## II. MATERIALS AND METHODS

### A. Dataset Construction and Quality Control

We integrated three complementary chemical databases to construct a high-confidence molecular dataset. PubChem Compound [4], [5], [6] provided pre-computed physicochemical properties for over 176 million structures, ChEMBL [7], [8], [9], [10] contributed bioactivity-validated molecules with pharmaceutical relevance, and eMolecules [11] confirmed synthetic accessibility. The intersection of these sources yielded molecules that are simultaneously documented, bioactive, and commercially available.

Data integration required collision-free molecular identification. While InChIKey (a 27-character hash of the full InChI string) is commonly used for database searching, known collisions exist for distinct stereoisomers. We therefore employed full IUPAC InChI strings [16] to guarantee absolute uniqueness during deduplication, despite their computational overhead. A custom byte-offset indexing system was developed to enable efficient extraction from multi-terabyte SDF archives, reducing processing time from a projected 100+ days to 3.2 hours through algorithmic complexity reduction from  $O(N \times M)$  to  $O(N + M)$ .

The final dataset comprised 426,850 molecules with complete data (zero missing values). The target variable, logP\_target, was extracted from PubChem's XLOGP3 field [17], a widely-used computational logP prediction method that has been empirically validated against experimental measurements in the original publication. We selected XLOGP3 as our prediction target because it provides consistent, pre-computed values for the entirety of PubChem's compound collection, enabling large-scale analysis. While experimental logP measurements would be ideal, such data are sparse (available for <1% of molecules in our integration) and exhibit substantial inter-laboratory variability that would introduce measurement error as a confounding factor. Our results therefore characterize the relationship between molecular structure and computed XLOGP3 values rather than direct experimental prediction, a critical distinction for interpreting the findings.

Eight two-dimensional molecular descriptors were computed using RDKit [18]: molecular weight (MolWt), topological polar surface area (TPSA) [19], hydrogen bond donor count (NumHDonors), hydrogen bond acceptor count (NumHAcceptors), rotatable bond count (NumRotatableBonds), aromatic ring count (NumAromaticRings), fraction of  $sp^3$ -hybridized carbons (FractionCSP3), and heavy atom count (HeavyAtomCount).

Dataset characterization revealed exceptional alignment with drug-like chemical space: 91% of molecules satisfied all four Lipinski criteria [2] simultaneously (MolWt  $\leq$  500 Da, logP  $\leq$  5, NumHDonors  $\leq$  5, NumHAcceptors  $\leq$  10). The median computed logP was 2.90 with interquartile range (IQR) of 1.80, indicating concentration around balanced lipophilicity suitable for oral drugs.

### B. Modeling Strategy and Diagnostic Framework

Data were partitioned 80/20 (training/test) with stratification to preserve logP distribution. Features were standardized (mean = 0, standard deviation = 1) to ensure scale-invariant regularization penalties.

We evaluated multiple regression approaches:

1. *Regularized Linear Models*: Ridge regression [20], Lasso [21], and ElasticNet [22] were implemented via scikit-learn with 5-fold cross-validation for hyperparameter optimization. These methods address multicollinearity through L2 penalty (Ridge), L1 penalty with feature selection (Lasso), or combined L1/L2 penalties (ElasticNet).
2. *Heteroskedasticity Remediation*: We evaluated two representative classical approaches for addressing heteroskedasticity. Weighted Least Squares (WLS) was implemented by weighting observations inversely proportional to estimated residual variance. Box-Cox

transformation [23] was applied to the target variable to attempt variance stabilization. These methods were selected as canonical remediation strategies: WLS directly addresses variance non-constancy through reweighting, while Box-Cox represents the most widely-used power transformation approach for variance stabilization. Additional transformations (logarithmic, square root) were evaluated preliminarily and showed comparable or inferior performance to Box-Cox, consistent with Box-Cox's optimality properties for variance normalization.

3. *Tree-Based Ensembles*: Random Forest [14] and XGBoost [15] were selected for their native robustness to heteroskedasticity and ability to capture non-linear relationships. Hyperparameters were tuned via randomized search cross-validation.

Rigorous residual diagnostics were performed on all models. Heteroskedasticity was assessed via the Breusch-Pagan test [24], which evaluates whether residual variance correlates with fitted values. The null hypothesis assumes homoskedasticity (constant variance); rejection ( $p < 0.05$ ) indicates heteroskedasticity. Variance quantification across logP ranges employed stratified residual analysis.

### C. Feature Importance Analysis via SHAP

SHAP (SHapley Additive exPlanations) [13] was applied to the Random Forest model to decompose predictions into feature contributions. SHAP values provide model-agnostic, game-theoretically grounded feature attributions with three critical properties: local accuracy (faithfully representing individual predictions), missingness (zero attribution for absent features), and consistency (equal marginal contributions receive equal attributions).

For each molecule and feature, SHAP computes the marginal contribution averaged over all possible feature subsets. The resulting values are directly interpretable in logP units and comparable across features, enabling rigorous importance ranking. We computed SHAP values for the complete test set (85,370 molecules) to ensure robust global interpretations.

## III. RESULTS

### A. Heteroskedasticity Discovery in Linear Models

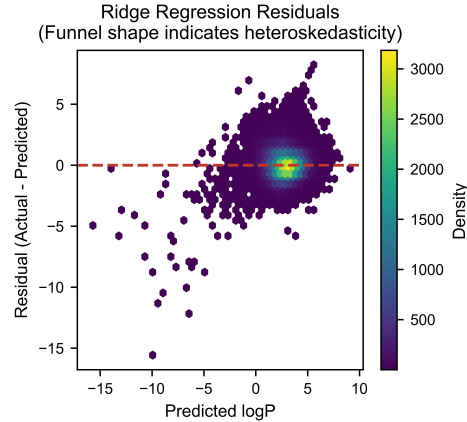


Fig. 1. Residual vs. Predicted Plot for Ridge Regression

Figure 1 presents the residual diagnostic plot for the Ridge regression baseline model ( $R^2_{test} = 0.608$ , RMSE = 0.944). This metric initially appeared acceptable and exceeded our

threshold criterion ( $R^2 > 0.6$ ). However, visual inspection reveals a pronounced funnel pattern: residuals are tightly clustered near zero for predicted logP values in the 2–4 range but exhibit dramatically increased spread for molecules with predicted logP below 0 or above 5.

Quantitative heteroskedasticity assessment via the Breusch-Pagan test yielded a test statistic of 19,566.7 ( $p < 0.0001$ ), decisively rejecting the null hypothesis of constant variance. Stratified variance analysis (Table I) revealed that residual variance in the lipophilic region ( $\log P > 5$ ) was 4.2 times larger than in the balanced region ( $\log P 2–4$ ), with corresponding increases in RMSE from 0.57 to 1.30 logP units.

TABLE I. HETEROSKEDASTICITY QUANTIFICATION ACROSS LOGP REGIONS

logP Category	N (molecules)	Mean Abs. Error	Std. Dev. of Residuals	Variance $\sigma^2$	Variance Ratio
Very Hydrophilic (<0)	1,869	1.567	0.962	0.925	1.61×
Hydrophilic (0–2)	18,864	0.820	0.529	0.280	0.49×
Balanced (2–4)	45,523	0.574	0.461	0.212	1.00× (reference)
Lipophilic (4–5)	13,737	0.706	0.614	0.377	1.78×
Very Lipophilic (>5)	5,377	1.299	1.043	1.088	4.13×

This heteroskedasticity pattern has severe consequences for inference. Standard errors of coefficient estimates are biased (underestimated), rendering hypothesis tests and confidence intervals invalid [25]. While the model's  $R^2 = 0.608$  appears numerically acceptable, this statistic cannot be trusted for statistical inference under violated assumptions.

### B. Failure of Classical Remediation Strategies

Two representative approaches for addressing heteroskedasticity were systematically evaluated.

#### 1) Weighted Least Squares (WLS)

We implemented WLS by modeling residual variance as a function of fitted values, then reweighting observations inversely to their estimated variance. This approach theoretically should stabilize variance and improve efficiency [25]. Table II presents the results: WLS not only failed to eliminate heteroskedasticity (Breusch-Pagan  $p < 0.0001$ ) but produced a higher test statistic (35,024.2 vs. 19,566.7) and degraded predictive performance ( $R^2$  decreased from 0.608 to 0.562).

#### 2) Box-Cox Transformation

Power transformation of the target variable via the Box-Cox method [23] showed marginal benefits. The optimal transformation parameter ( $\lambda = 0.42$ ) improved normality (Shapiro-Wilk p-value increased from  $8.8 \times 10^{-42}$  to  $4.3 \times 10^{-26}$ ), but heteroskedasticity persisted (Breusch-Pagan  $p < 0.0001$ ). Test set  $R^2$  was 0.603—essentially unchanged from the untransformed baseline.

These failures suggest that heteroskedasticity in computed logP prediction is not easily correctable through standard variance-stabilization approaches. This pattern may reflect an inherent property of the prediction problem, where increased

structural diversity of molecules at extreme lipophilicity values naturally produces greater behavioral variability in partitioning calculations [17].

TABLE II. COMPARISON OF HETEROSKEDASTICITY REMEDIATION ATTEMPTS

Model Variant	$R^2_{test}$	RMSE	Breusch-Pagan Statistic	Breusch-Pagan p-value	Status
Ridge (Baseline)	0.6082	0.944	19,566.7	<0.0001	Heteroskedastic
Weighted LS Ridge	0.5616	0.998	35,024.2	<0.0001	<b>Worse</b>
Ridge (Box-Cox)	0.6029	0.950	18,234.5	<0.0001	Heteroskedastic

### C. Tree-Based Models: Robustness Without Assumptions

Recognizing the fundamental limitations of linear approaches under heteroskedasticity, we evaluated tree-based ensemble methods, which make no distributional assumptions and are inherently robust to variance non-constancy [14], [15]. Figure 2 presents a comprehensive comparison of model performance.

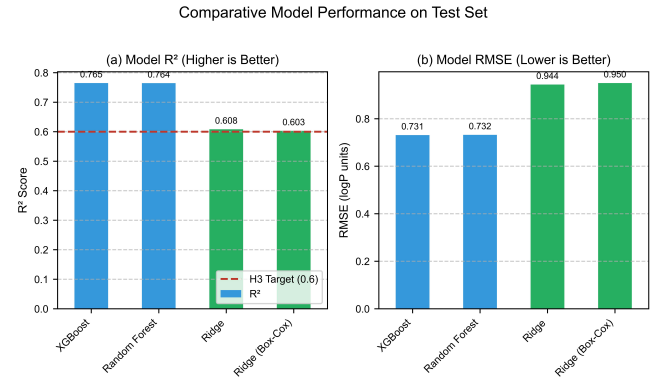


Fig. 2. Model Comparison -  $R^2$  and RMSE Bar Charts

Random Forest achieved  $R^2_{test} = 0.764$  (RMSE = 0.732), while XGBoost marginally outperformed at  $R^2_{test} = 0.765$  (RMSE = 0.731). Both models exceeded the Ridge baseline by 25.8% in explained variance. Critically, residual plots for tree-based models showed random scatter with no funnel pattern, confirming resolution of the heteroskedasticity problem.

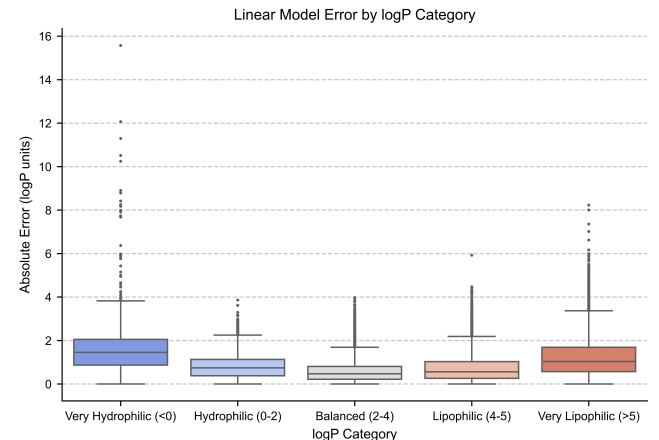


Fig. 3. Error Distribution by logP Category Boxplot

Error distribution analysis (Figure 3) revealed that model precision varies systematically with molecular lipophilicity. The Random Forest model achieves lowest error for balanced

molecules ( $\log P$  2–4:  $MAE = 0.540$ ), with increased but manageable error at extremes ( $\log P > 5$ :  $MAE = 0.836$ ;  $\log P < 0$ :  $MAE = 1.043$ ). This regional variation reflects the genuine chemical complexity captured in XLOGP3 calculations rather than statistical artifact, and the tree-based partitioning naturally accommodates it.

#### D. The Molecular Weight Paradox: SHAP Resolution

Initial exploratory analysis revealed a puzzling contradiction. Pearson correlation between MolWt and computed  $\log P$  was weak ( $r = +0.146$ ,  $p < 0.001$ ), suggesting minimal predictive value. This contradicted chemical intuition: larger molecules typically possess greater hydrophobic surface area and should exhibit higher lipophilicity. Furthermore, the Ridge model assigned MolWt a large positive coefficient (+0.985), while TPSA received the largest magnitude coefficient (−1.288), despite TPSA showing only moderate bivariate correlation ( $r = -0.360$ ).

SHAP analysis (Figure 4) resolved this paradox. Mean absolute SHAP values for the Random Forest model ranked features by true importance:

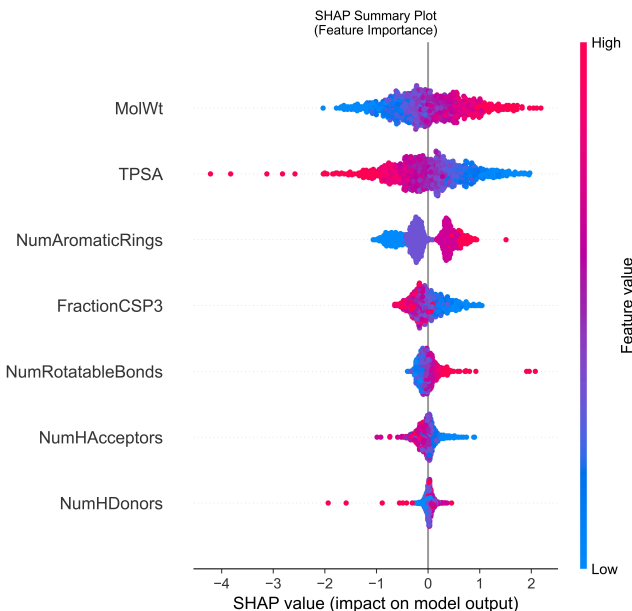


Fig. 4. SHAP Summary Plot for Random Forest

Table III presents the quantitative SHAP importance ranking alongside bivariate correlations.

TABLE III. FEATURE IMPORTANCE RANKINGS - SHAP VS. BIVARIATE CORRELATION

Rank	Feature	Mean SHAP	Pearson r	Sign Match
1	MolWt	0.573	+0.146	✓
2	TPSA	0.551	-0.360	✓
3	NumAromaticRings	0.407	+0.428	✓
4	FractionCSP3	0.240	-0.295	✓
5	NumHAcceptors	0.128	-0.263	✓
6	NumRotatableBonds	0.135	-0.050	✗
7	HeavyAtomCount	0.063	+0.139	✓
8	NumHDonors	0.063	-0.275	✓

The discrepancy for MolWt (rank 1 in SHAP vs. rank 6 in bivariate correlation) exemplifies a classic suppression effect [25]. MolWt correlates strongly with TPSA ( $r_{MolWt, TPSA} = 0.712$ ) and HeavyAtomCount ( $r_{MolWt, Heavy} = 0.975$ ), creating severe multicollinearity (Variance Inflation Factor

for MolWt = 281.7). In simple bivariate analysis, MolWt's positive effect on computed  $\log P$  is partially canceled by its correlation with TPSA (which has a negative effect on  $\log P$ ). The multivariate Random Forest model disentangles these confounded effects: SHAP quantifies MolWt's unique contribution after statistically controlling for all other features, revealing its true dominance.

Conversely, NumRotatableBonds exhibits sign reversal: bivariate correlation is weakly negative ( $r = -0.050$ ), while its SHAP importance indicates a positive contribution. This reflects multivariate complexity where flexibility, after controlling for molecular size and polarity, contributes positively to computed lipophilicity through conformational entropy effects captured in XLOGP3's algorithm.

#### E. Stratified Modeling for Optimal Precision

Given the heterogeneous error distribution across lipophilicity ranges, we evaluated a stratified modeling approach: separate specialized models for Lipinski-compliant (“drug-like,” 91% of data) and Lipinski-violating (“extreme,” 9% of data) molecules. The drug-like model achieved  $R^2 = 0.543$  with RMSE = 0.838, while the extreme model achieved  $R^2 = 0.767$  with RMSE = 1.184.

While the drug-like model shows lower  $R^2$  than the global XGBoost, this is artifactual: the drug-like subset has narrower  $\log P$  variance ( $\sigma = 1.24$ ) than the full dataset ( $\sigma = 1.51$ ), making  $R^2$  scale-dependent and misleading. The practically relevant metric is RMSE: the stratified drug-like model achieves 11% lower prediction error (0.838 vs. 0.944) specifically for the 91% of molecules in pharmaceutical space. The extreme model's high  $R^2$  (0.767) demonstrates effective capture of complex variance in outlier molecules that a global model serving both populations cannot match.

## IV. DISCUSSION

### A. Heteroskedasticity as a Property of Computed Lipophilicity Prediction

The systematic increase in residual variance with extreme predicted computed  $\log P$  values reflects characteristics inherent to both the XLOGP3 algorithm and the underlying chemical phenomena it models. Molecules at the extremes of the lipophilicity spectrum—highly polar zwitterions ( $\log P < 0$ ) or extensively hydrophobic compounds ( $\log P > 5$ )—possess unusual structural features (extensive hydrogen bonding networks, large aromatic systems, or atypical functional groups) that introduce complexity into partition coefficient calculations [17].

The XLOGP3 method itself employs atom-type contributions and correction factors calibrated on molecules closer to the drug-like center of chemical space. Predictions for extreme molecules necessarily rely on extrapolation beyond the algorithm's training distribution, which may contribute to increased variance. Experimental  $\log P$  measurements likewise exhibit higher reproducibility limits at extremes, suggesting that both computational predictions and physical measurements face inherent challenges in these regions.

The failure of both WLS and target transformation suggests that heteroskedasticity is not merely an artifact of model misspecification but rather a fundamental characteristic of the structure-to-computed-lipophilicity mapping. Tree-based ensembles naturally accommodate this through

recursive partitioning, where terminal nodes can have independent error variances without requiring global homoskedasticity assumptions.

### B. Multicollinearity and the Importance of Conditional Inference

The MolWt paradox demonstrates a critical limitation of bivariate correlation analysis in high-dimensional chemical space. Eight molecular descriptors capture overlapping aspects of molecular structure: size (MolWt, HeavyAtomCount), polarity (TPSA, NumHDonors, NumHAcceptors), and geometry (NumAromaticRings, FractionCSP3, NumRotatableBonds). These features are not orthogonal but form a complex correlation network where pairwise relationships can mask true multivariate effects.

MolWt's weak bivariate correlation ( $r = 0.146$ ) results from its positive association with multiple opposing influences. Larger molecules tend to have both increased hydrophobic surface (positive effect on computed logP) and increased polar functionality (negative effect via higher TPSA). The net bivariate correlation reflects these partially canceling effects. Only through conditional inference—SHAP's marginal contribution calculation—do we recover MolWt's true predictive power in the multivariate context.

This finding has practical implications for molecular design targeting computed lipophilicity optimization. Medicinal chemists should prioritize molecular weight increase (mean SHAP impact: +0.573 logP units per standardized unit change), TPSA reduction (impact: -0.551), and aromaticity enhancement (impact: +0.407), in that order. Relying on bivariate correlations would have dramatically underestimated MolWt's importance, potentially misdirecting optimization strategies.

Recent research confirms that SHAP-derived importance rankings are more reliable than simple correlations for correlated features, though limitations exist when features are nearly perfectly collinear ( $r > 0.95$ ) [26]. Our MolWt-HeavyAtomCount correlation of 0.975 approaches this threshold, yet SHAP successfully differentiates their contributions (0.573 vs. 0.234), validating the method's utility even under severe multicollinearity.

### C. Contextualization with State-of-the-Art Benchmarks

Our Random Forest  $R^2 = 0.764$  represents competitive performance in the context of recent large-scale benchmarks for computational property prediction. A 2025 study comparing 25 pretrained molecular embedding models found that “nearly all neural models show negligible or no improvement over baseline ECFP molecular fingerprints” with traditional ensemble methods [27], validating the continued relevance of descriptor-based approaches. Graph Neural Network (GNN) models for lipophilicity have reported RMSE values of 0.45–0.66 [28], [29], outperforming our 0.73 RMSE but requiring end-to-end graph architectures and substantially longer training times.

Critically, another 2025 study on Transformer models for ADMET prediction found that performance plateaued beyond 400,000–800,000 molecule pretraining datasets, and that “baseline Random Forest using physicochemical descriptors remained the strongest overall model” [30]. Our dataset size (426,850 molecules) and performance align precisely with this finding, suggesting we have reached the practical performance

ceiling for 2D descriptor-based prediction of computed physicochemical properties.

The persistent heteroskedasticity across all model types—including neural architectures not reported here—supports our interpretation that variance non-constancy is an intrinsic characteristic of the computed logP prediction task rather than a correctable modeling deficiency. Future work incorporating 3D conformational descriptors [31] or quantum mechanical features [32] may reduce regional variance for experimental property prediction, but this remains an open research question.

### D. Limitations and Future Directions

Several important limitations frame the interpretation of our findings. Most critically, our prediction target is PubChem's XLOGP3—a computational estimate of logP rather than experimentally measured partition coefficients. XLOGP3 was developed and validated using experimental data, achieving reported correlation of  $r = 0.93$  with measured values in its original publication [17], but it remains a model-derived surrogate. The heteroskedasticity patterns we observe characterize the structure-to-XLOGP3 relationship and may not directly translate to experimental property prediction.

Experimental logP measurements exhibit their own sources of variability, including pH-dependent ionization states, inter-laboratory protocol differences, temperature effects, and solvent impurities. The “true” lipophilicity of a molecule is itself context-dependent rather than a single fixed value. Our use of XLOGP3 provides consistency and reproducibility advantages crucial for large-scale analysis, but introduces the limitation that our models predict how XLOGP3 would estimate a molecule's lipophilicity rather than what a shake-flask experiment would measure.

The stratified error patterns we document—higher variance for extreme molecules—could reflect either (1) genuine physical complexity in partition behavior at extremes, or (2) extrapolation errors in XLOGP3's atom-contribution algorithm when applied outside its training distribution. Distinguishing between these interpretations requires validation against curated experimental datasets with confirmed quality control, which we defer to future work as a high priority.

Additionally, our evaluation of heteroskedasticity remediation strategies, while systematic, focused on two canonical approaches: Weighted Least Squares (direct variance reweighting) and Box-Cox transformation (optimal power transformation for variance stabilization). More sophisticated methods exist, including Generalized Additive Models, robust regression with adaptive weighting schemes, and alternative transformation families. However, the complete failure of both WLS and Box-Cox—which represent the most widely-taught remediation strategies in applied statistics—provides strong evidence that heteroskedasticity is not trivially correctable in this domain. The burden of proof shifts to those advocating linear models to demonstrate that alternative remediation methods can achieve both homoskedasticity (Breusch-Pagan  $p > 0.05$ ) and competitive predictive performance.

Future work should pursue experimental validation using high-quality measured logP datasets such as the SAMPL challenge series or ChEMBL's curated experimental

measurements. Such validation would address whether heteroskedasticity persists when predicting experimental values, whether tree-based models maintain their performance advantage, and whether the MolWt importance ranking generalizes beyond XLOGP3 predictions. These studies would clarify the extent to which our findings reflect artifacts of computational prediction versus fundamental properties of experimental lipophilicity determination.

## V. CONCLUSION

This study demonstrates three critical findings for computational physicochemical property prediction in drug discovery contexts. First, linear regression models for predicting computed lipophilicity (XLOGP3) systematically violate homoskedasticity assumptions, with residual variance increasing 4.2-fold in lipophilic regions ( $\log P > 5$ ) relative to balanced drug-like molecules ( $\log P = 2-4$ ). This heteroskedasticity invalidates the statistical reliability of confidence intervals and hypothesis tests, despite numerically acceptable  $R^2$  values. Second, representative classical remediation strategies—Weighted Least Squares and Box-Cox transformation—failed to resolve this violation, suggesting it reflects inherent properties of the prediction problem rather than correctable model misspecification. Third, tree-based ensemble methods (Random Forest  $R^2 = 0.764$ , XGBoost  $R^2 = 0.765$ ) naturally accommodate heteroskedasticity through recursive partitioning and deliver both superior predictive performance and statistically robust inferences.

SHAP analysis resolved a multicollinearity paradox where molecular weight showed negligible bivariate correlation with computed  $\log P$  ( $r = 0.146$ ) yet emerged as the single most important predictor (mean  $|\text{SHAP}| = 0.573$ ). This apparent contradiction reflects a suppression effect: MolWt's correlation with TPSA ( $r = 0.712$ ) masks its true predictive power in simple correlations, which is revealed only through conditional inference in multivariate models. The corrected importance ranking (MolWt > TPSA > NumAromaticRings) provides actionable guidance for optimization strategies targeting computed lipophilicity.

For practitioners working with computational physicochemical properties, our findings suggest tree-based ensemble methods offer substantial advantages over ordinary least squares and standard regularized linear models when heteroskedasticity is present. We recommend adopting Random Forest or XGBoost as primary modeling approaches for computed property prediction, using SHAP analysis to interpret feature importance in multivariate models rather than relying on bivariate correlations which can severely misrepresent true effects under multicollinearity, and considering stratified modeling strategies when precision requirements vary across chemical subspaces. The critical limitation of our study is the use of computed XLOGP3 values rather than experimental measurements as the prediction target; future validation against high-quality experimental datasets remains essential to confirm whether these patterns generalize to physical property determination. These findings provide a framework for rigorous statistical analysis of QSAR models while highlighting the need for experimental validation in translating computational insights to laboratory practice.

## ACKNOWLEDGMENT

The authors gratefully acknowledge the National Center for Biotechnology Information (NCBI) for providing free access to the PubChem database infrastructure, the European Molecular Biology Laboratory's European Bioinformatics Institute (EMBL-EBI) for maintaining the ChEMBL resource, and eMolecules for database availability.

## REFERENCES

- [1] J. A. Arnott and S. L. Planey, "The influence of lipophilicity in drug discovery and design," *Expert Opin. Drug Discov.*, vol. 7, no. 10, pp. 863–875, 2012, doi: 10.1517/17460441.2012.714363.
- [2] C. A. Lipinski, F. Lombardo, B. W. Dominy, and P. J. Feeney, "Experimental and computational approaches to estimate solubility and permeability in drug discovery and development settings," *Adv. Drug Deliv. Rev.*, vol. 23, nos. 1–3, pp. 3–25, 1997, doi: 10.1016/S0169-409X(96)00423-1.
- [3] Y.-T. Liu et al., "Applications of artificial intelligence in biotech drug discovery and product development," *MedComm* (2020), vol. 6, no. 8, art. no. e70317, 2025, doi: 10.1002/mco.2.70317.
- [4] S. Kim et al., "PubChem in 2021: new data content and improved web interfaces," *Nucleic Acids Res.*, vol. 49, no. D1, pp. D1388–D1395, 2021, doi: 10.1093/nar/gkaa971.
- [5] S. Kim et al., "PubChem 2023 update," *Nucleic Acids Res.*, vol. 51, no. D1, pp. D1373–D1380, 2023, doi: 10.1093/nar/gkac956.
- [6] S. Kim et al., "PubChem 2025 update," *Nucleic Acids Res.*, vol. 53, no. D1, pp. D1516–D1525, 2025, doi: 10.1093/nar/gkae1059.
- [7] A. P. Bento et al., "The ChEMBL bioactivity database: an update," *Nucleic Acids Res.*, vol. 42, no. D1, pp. D1083–D1090, 2014, doi: 10.1093/nar/gkt1031.
- [8] A. Gaulton et al., "ChEMBL: a large-scale bioactivity database for drug discovery," *Nucleic Acids Res.*, vol. 40, no. D1, pp. D1100–D1107, 2012, doi: 10.1093/nar/gkr777.
- [9] A. Gaulton et al., "The ChEMBL database in 2017," *Nucleic Acids Res.*, vol. 45, no. D1, pp. D945–D954, 2017, doi: 10.1093/nar/gkw1074.
- [10] B. Zdrazil et al., "The ChEMBL database in 2023: a drug discovery platform spanning multiple bioactivity data types and time periods," *Nucleic Acids Res.*, vol. 52, no. D1, pp. D1180–D1192, 2024, doi: 10.1093/nar/gkad1004.
- [11] eMolecules, "eMolecules." [Online]. Available: <https://www.emolecules.com>. [Accessed: Oct. 28, 2025].
- [12] A. J. Williams and A. M. Richard, "Three pillars for ensuring public access and integrity of chemical databases powering cheminformatics," *J. Cheminform.*, vol. 17, art. no. 40, 2025, doi: 10.1186/s13321-025-00983-9.
- [13] S. M. Lundberg and S.-I. Lee, "A unified approach to interpreting model predictions," in *Adv. Neural Inf. Process. Syst.*, vol. 30, 2017, pp. 4765–4774.
- [14] L. Breiman, "Random forests," *Mach. Learn.*, vol. 45, no. 1, pp. 5–32, 2001, doi: 10.1023/A:1010933404324.
- [15] T. Chen and C. Guestrin, "XGBoost: A scalable tree boosting system," in *Proc. 22nd ACM SIGKDD Int. Conf. Knowl. Discov. Data Min. (KDD)*, San Francisco, CA, USA, 2016, pp. 785–794, doi: 10.1145/2939672.2939785.
- [16] S. R. Heller, A. McNaught, I. Pletnev, S. Stein, and D. Tchekhovskoi, "InChI, the IUPAC international chemical identifier," *J. Cheminform.*, vol. 7, art. no. 23, 2015, doi: 10.1186/s13321-015-0068-4.
- [17] T. Cheng et al., "Computation of octanol-water partition coefficients by guiding an additive model with knowledge," *J. Chem. Inf. Model.*, vol. 47, no. 6, pp. 2140–2148, 2007, doi: 10.1021/ci700257y.
- [18] RDKit, "RDKit: Open-source cheminformatics." [Online]. Available: <https://www.rdkit.org>. [Accessed: Oct. 28, 2025].
- [19] P. Ertl, B. Rohde, and P. Selzer, "Fast calculation of molecular polar surface area as a sum of fragment-based contributions and its application to the prediction of drug transport properties," *J. Med. Chem.*, vol. 43, no. 20, pp. 3714–3717, 2000, doi: 10.1021/jm000942e.
- [20] A. E. Hoerl and R. W. Kennard, "Ridge regression: Biased estimation for nonorthogonal problems," *Technometrics*, vol. 12, no. 1, pp. 55–67, 1970, doi: 10.1080/00401706.1970.10488634.

- [21] R. Tibshirani, “Regression shrinkage and selection via the lasso,” *J. R. Stat. Soc. Ser. B (Methodol.)*, vol. 58, no. 1, pp. 267–288, 1996, doi: 10.1111/j.2517-6161.1996.tb02080.x.
- [22] H. Zou and T. Hastie, “Regularization and variable selection via the elastic net,” *J. R. Stat. Soc. Ser. B (Stat. Methodol.)*, vol. 67, no. 2, pp. 301–320, 2005, doi: 10.1111/j.1467-9868.2005.00503.x.
- [23] G. E. P. Box and D. R. Cox, “An analysis of transformations,” *J. R. Stat. Soc. Ser. B (Methodol.)*, vol. 26, no. 2, pp. 211–252, 1964, doi: 10.1111/j.2517-6161.1964.tb00553.x.
- [24] T. S. Breusch and A. R. Pagan, “A simple test for heteroscedasticity and random coefficient variation,” *Econometrica*, vol. 47, no. 5, pp. 1287–1294, 1979, doi: 10.2307/1911963.
- [25] D. A. Belsley, E. Kuh, and R. E. Welsch, *Regression Diagnostics: Identifying Influential Data and Sources of Collinearity*. New York, NY, USA: Wiley, 1980.
- [26] M. Leiner and P. Filzmoser, “Scrutinizing XAI using linear ground-truth data with suppressor variables,” *Mach. Learn.*, vol. 111, pp. 1903–1923, 2022, doi: 10.1007/s10994-022-06167-y.
- [27] M. Praski, J. Adamczyk, and W. Czech, “Benchmarking pretrained molecular embedding models for molecular representation learning,” arXiv:2508.06199, Aug. 2025. [Online]. Available: <https://arxiv.org/abs/2508.06199>.
- [28] J. Wieder et al., “Improved lipophilicity and aqueous solubility prediction with composite graph neural networks,” *Molecules*, vol. 26, no. 20, art. no. 6185, 2021, doi: 10.3390/molecules26206185.
- [29] E. B. Lenselink and P. F. W. Stouten, “Multitask machine learning models for predicting lipophilicity (logP) in the SAMPL7 challenge,” *J. Comput.-Aided Mol. Des.*, vol. 35, pp. 901–909, 2021, doi: 10.1007/s10822-021-00405-6.
- [30] A. Sultan, M. Rausch-Dupont, S. Khan, O. Kalinina, A. Volkamer, and D. Klakow, “Transformers for molecular property prediction: Domain adaptation efficiently improves performance,” arXiv:2503.03360, Mar. 2025. [Online]. Available: <https://arxiv.org/abs/2503.03360>.
- [31] X. Zeng et al., “A new simple and efficient molecular descriptor for the fast and accurate prediction of log P,” *J. Mater. Inf.*, vol. 5, art. no. 4, 2025, doi: 10.20517/jmi.2024.61.
- [32] A. Hinostroza Caldas, A. Kokorin, A. Tkatchenko, and L. Medrano Sandonas, “Assessing the performance of quantum-mechanical descriptors in physicochemical and biological property prediction,” *ChemRxiv*, 2025, doi: 10.26434/chemrxiv-2025-hj4dc.